Respiratory Sinus Arrhythmia in Dogs

Effects of Phasic Afferents and Chemostimulation

B. E. Shykoff, S. S. J. Naqvi, A. S. Menon, and A. S. Slutsky
Departments of Medicine and Research, Mount Sinai Hospital, University of Toronto, Ontario M5G1X5 Canada

Abstract

We examined the hypothesis that respiratory sinus arrhythmia (RSA) is primarily a central phenomenon and thus that RSA is directly correlated with respiratory controller output. RSA was measured in nine anesthetized dogs, first during spontaneous breathing (SB) and then during constant flow ventilation (CFV), a technique whereby phasic chest wall movements and thoracic pressure swings are eliminated. Measurements of the heart rate and of the moving time averaged (MTA) phrenic neurogram during these two ventilatory modes were made during progressive hypercapnia and progressive hypoxia. RSA divided by the MTA phrenic amplitude (RSA_a) showed a power-law relationship with both arterial carbon dioxide partial pressure ($Paco_2$) and oxygen saturation (Sa_{O_2}), but with different exponents for different conditions. However, the power-law relation between RSA_a and respiratory frequency had an exponent indistinguishable from −2 whether hypoxia or hypercapnia was the stimulus for increased respiratory drive, and during both CFV and spontaneous breathing (−1.9±0.4, hypoxia, SB; −1.8±0.7, hypoxia, CFV; −2.1±0.8, hypercapnia, SB; −1.9±0.7, hypercapnia, CFV). We conclude that respiratory sinus arrhythmia is centrally mediated and directly related to respiratory drive, and that changes in blood gases and phasic afferent signals affect RSA primarily by influencing respiratory drive. (*J. Clin. Invest.* 1991. 87:1621–1627.) Key words: heart rate · pulmonary reflexes · mathematical modeling · constant flow ventilation · hypoxia

Introduction

The modulation of the heart rate in time with breathing, usually known as respiratory sinus arrhythmia (RSA),[1] has been the focus of many studies since its first description (1). Although it is well accepted that the efferent pathway is almost entirely vagal both in dogs (2) and in man (3), mechanisms responsible for the rhythmic changes in heart rate are only partially understood. Among those that have been proposed are the atrial or vascular baro- or mechanoreceptor responses to intrathoracic pressure changes, pulmonary stretch receptor afferent signals, and direct projection in the brain stem from the respiratory center onto the nuclei that govern heart rate or blood pressure.

A number of factors have been shown to modify the magnitude of the respiratory modulation including chemoreceptor stimulation (3, 4), tidal volume (3, 5, 6), and respiratory rate (3, 6, 7), with the rate dependence showing low-pass, but not necessarily linear, behavior. In this study we set out to investigate a unifying hypothesis that could explain the modulation of heart rate with these ventilatory variables. We hypothesized that the primary mechanism mediating the respiratory modulation of heart rate is central projection from the respiratory controller, and thus that RSA is directly correlated with respiratory drive. We postulated, therefore, that the differences in RSA observed during hypoxia and hypercapnia (3, 4) are not directly related to chemical stimulation but rather to the changes in respiratory drive induced by the changes in arterial blood gases.

We measured RSA in both the presence (during spontaneous breathing) and absence of phasic afferent signals from the chest wall and vagus during progressive hypoxia and hypercapnia. To eliminate the phasic changes in pleural pressure and pulmonary vagal inputs and the respiratory oscillations of arterial blood gases (8), we used a ventilatory technique known as constant flow ventilation (CFV) (9–11). Using CFV, arterial blood gases can be manipulated while the lungs and chest wall do not move. The steady afferent signals remain but phasic feedback is removed. Thus, we were able to study the effect of hypoxic and hypercapnic stimulation with and without the phasic changes in peripheral afferent stimulation caused by tidal ventilation. As our measure of central respiratory drive, we measured the moving time average phrenic neurogram. Our hypothesis led us to expect that RSA would correlate strongly with the phrenic neurogram, irrespective of the arterial blood gases or the mode of ventilation.

Methods

Nine dogs of mixed breed weighing between 18 and 30 kg were used. The dogs were medicated with fentanyl and droperidol and anesthetized with intravenous chloralose-urethane. Anesthesia was induced with a loading dose of 0.8 ml/kg chloralose-urethan solution i.v. (2.5 g chloralose plus 25 g urethane in 100 ml saline), and sustained with supplementary doses of ~ 0.3 ml/kg/h. Pedal and corneal reflexes were examined frequently during spontaneous breathing runs to monitor the adequacy of anesthesia, and the same dose and schedule of anesthetic was continued after the animal was paralyzed for CFV. Paralysis was induced and maintained with metubine iodide, 0.2 mg/kg/h intravenously.

Phrenic nerve activity was recorded from the C6 cervical root of the phrenic nerve using a copper electrode held in place with a silicone based elastomeric impression material (Reprosil; De Trey, Dentsply, Surrey, UK). The nerve was bathed intermittently in mineral oil to prevent it from drying. The signals from the nerve were amplified (gain:

Address reprint requests to Dr. Arthur S. Slutsky, Mount Sinai Hospital, 600 University Avenue, #656A, Toronto, Ontario M5G 1X5, Canada.

Received for publication 15 August 1990 and in revised form 30 November 1990.

1. *Abbreviations used in this paper:* CFV, constant flow ventilation; FM, frequency modulation; MTA, moving time averaged; RSA, respiratory sinus arrhythmia; RSA_a, RSA divided by the MTA phrenic amplitude; SB, spontaneous breathing.

J. Clin. Invest.

0021-9738/91/05/1621/07 $2.00
Volume 87, May 1991, 1621–1627

200,000) band pass filtered (low half-amplitude frequency, 100 Hz; high half-amplitude frequency, 10 kHz) (P511K AC preamplifier; Grass Instruments Co., Quincy, MA), and passed through a contour follower with a time constant of 70 ms (Contour Following Integrator; Coulbourn Instruments Inc., Lehigh Valley, PA). The signals were full-wave rectified and low-pass filtered to yield the moving time average (MTA) signal.

The animals were intubated with a midcervical tracheostomy. Femoral arterial and venous catheters were placed to monitor pressure, to administer drugs and fluids, and to draw blood samples. Arterial blood pressure was measured using a catheter-transducer system (PD 23; Gould Inc., Instruments Div., Santa Clara, CA). Beat-by-beat heart rate was obtained from the blood pressure pulse interval (Biotach amplifier; Gould Inc., Medical Products Div., Oxnard, CA). Blood gas partial pressures were obtained by analysis of 0.8 ml aliquots of arterial blood (model 168 analyzer; Corning Medical and Scientific, Corning Glass Works, Medford, MA). Esophageal pressure was measured using a pressure transducer (MP 45-30; Validyne Engineering Corp., Northridge, CA) connected to an esophageal balloon. Arterial oxygen saturation (SaO_2) was monitored using an oximeter probe (Biox II; Ohmeda, Boulder, CO) placed on the dog's tongue. Rectal temperature was monitored by a probe (Yellow Springs Instrument Co., Yellow Springs, OH), and a heated surgical table was used to maintain normothermia.

Selected mixtures of O_2, N_2, and CO_2 were obtained using a mass flow controller (multiple dynablender model 8249; Matheson Gas Products, Inc., Secaucus, NJ) to feed metered amounts of the individual gases into a common line. The gas mixture was heated to ~ 40°C by passing it through coils immersed in a hot water bath. The expired carbon dioxide concentration was monitored at the airway opening using an infrared analyzer (LB2; Sensor Medics, Anaheim, CA).

During the spontaneous breathing measurements the dogs breathed through a cuffed tracheostomy tube connected with a T-piece to a "blow by " circuit through which the constant flow of the gas mixture from the flow controller was delivered. The cuff of the tracheostomy tube was deflated after the spontaneous breathing experiments were completed. The constant flow delivery system was then placed with the supporting tubes cradling the carina (10, 11), and the constant flow insufflation catheters (1.67 mm i.d.) were advanced until their tips were ~ 3 cm distal to the carina, one in each mainstem bronchus. The position of the catheters was confirmed by fiberoptic bronchoscopy and the cuff on the tracheostomy tube was reinflated to hold the CFV assembly in place. A constant flow of gas from the controller was delivered to the catheters at a rate sufficient to maintain normocapnia and normoxia with the control gas mixture. The total flows used ranged from 20 to 40 liters/min.

Experimental protocol

Progressive normocapnic hypoxia was induced after a normoxic normocapnic steady state (P_aCO_2: 35–40 Torr) was established. The O_2 flow was decreased and the N_2 flow increased using the flow controller while the dog breathed spontaneously from the blow by circuit. The end tidal carbon dioxide partial pressure ($P_{ET}CO_2$) was maintained between 37 and 39 Torr by adding carbon dioxide to the inspired gas. Gas concentration changes were made at a rate such that an SaO_2 of ~ 60% was reached in 8–10 min. An arterial blood sample was drawn to monitor the blood gas status for every 5% decrease in SaO_2 as measured with the oximeter.

The baseline blood gas values were restored after the spontaneous breathing normocapnic hypoxic run was completed by adjusting the mixture of inspired gases to approximate room air. It took 15–20 min for the return to a normocapnic, normoxic steady state. Progressive hyperoxic hypercapnia was then induced by replacing the nitrogen in the breathing mixture with oxygen and by gradually increasing the inspired carbon dioxide concentration. The $PaCO_2$ rose to 70 Torr in ~ 8–10 min.

The baseline blood gas values were restored again after the spontaneous breathing hypercapnic run was completed by adjusting the mixture of inspired gases to approximate room air. The CFV system then was positioned as described above and the animal was paralyzed by a slow infusion of metubine iodide. Esophageal pressure (P_{es}) was monitored both as an indicator of mean lung volume and to confirm that the dog was not breathing during the CFV runs.

Progressive hypoxia was induced as in the spontaneous breathing run after a normoxic, normocapnic steady state was attained with CFV. The total flow of gas delivered was held constant while the composition was adjusted (decreased O_2 and increased N_2). The blood gases were then returned to normal by readjusting the gas mixture, and progressive hyperoxic hypercapnia was induced and monitored during CFV.

The MTA phrenic neurogram, SaO_2, heart rate, arterial and esophageal pressures, and expired carbon dioxide partial pressure were obtained continuously and recorded on paper (ES1000 electrostatic recorder; Gould, Inc.) during the experiments.

Data analysis

The recorded data were digitized (Super-grid digitizer; Summagraphics Corp., Fairfield, CT) for analysis. The beginning of inspiratory activity and the time of the peak of the MTA phrenic neurogram were defined to be the onset of inspiration and of expiration, respectively (Fig. 1). The inspiratory time (Ti), expiratory time (Te), and amplitude were measured from the record of the MTA phrenic neurogram for five bursts ("breaths") for every 5% drop in SaO_2 during a progressive hypoxia experiment and every 2 min during a progressive hypercapnia experiment. Maximum and minimum heart rates were measured for each of the five phrenic bursts, and the difference between them taken as the value of RSA. The data for the five breaths were averaged.

Since oximeters tend to underestimate the SaO_2 calculated from blood gas measurements (12), the oximeter values were corrected using a regression equation determined using arterial blood gases obtained simultaneously with some of the readings (13).

The RSA for the five breaths was divided by the average height of the five corresponding MTA phrenic neurogram bursts to yield the adjusted RSA amplitude, RSA_a. Bode plots (log variable vs. log respiratory frequency plots) were constructed for the individual experiments and regression lines were calculated to obtain the roll-off slopes.

Inspection of the Bode plots led to RSA_a being considered as a second order system. The parameters for the four experimental conditions (CFV, SB, hypoxia, hypercapnia) were obtained by pooling the frequency responses for the individual dogs. To compare results among dogs, the data were normalized by dividing RSA_a by the RSA_a amplitude at 10 breaths/min. The time constant of the first exponential term was found from the intersection of the 0 dB/decade slope and the −20 dB/decade slope asymptotes, and that of the second from the intersection of the −20 dB/decade slope and the −40 dB/decade slope asymptote. The natural frequency was calculated as the geometric mean of the inverse of the time constants and was confirmed to correspond to the intersection of the −40 dB/decade and the 0 dB/decade slope asymptotes. The damping parameter was calculated as the product of the natural frequency and the arithmetic mean of the time constants.

Results

A sample of raw data is shown in Fig. 1, with the onset of inspiration and expiration marked. The respiratory sinus arrhythmia is clearly evident on the record of beat-to-beat heart rate. The magnitude of RSA observed in all the runs ranged from 10 to 60 bpm. Mean heart rates ranged from ~ 80 to ~ 200 bpm, but were generally in the 120–130 bpm range. Mean arterial pressures remained fairly steady, with mean increases of < 20 mmHg in all runs.

Sample plots of RSA_a against $PaCO_2$ or SaO_2 and their log–log representation are shown in Fig. 2. Although there were inverse power law relations (linear log–log plots) between RSA_a

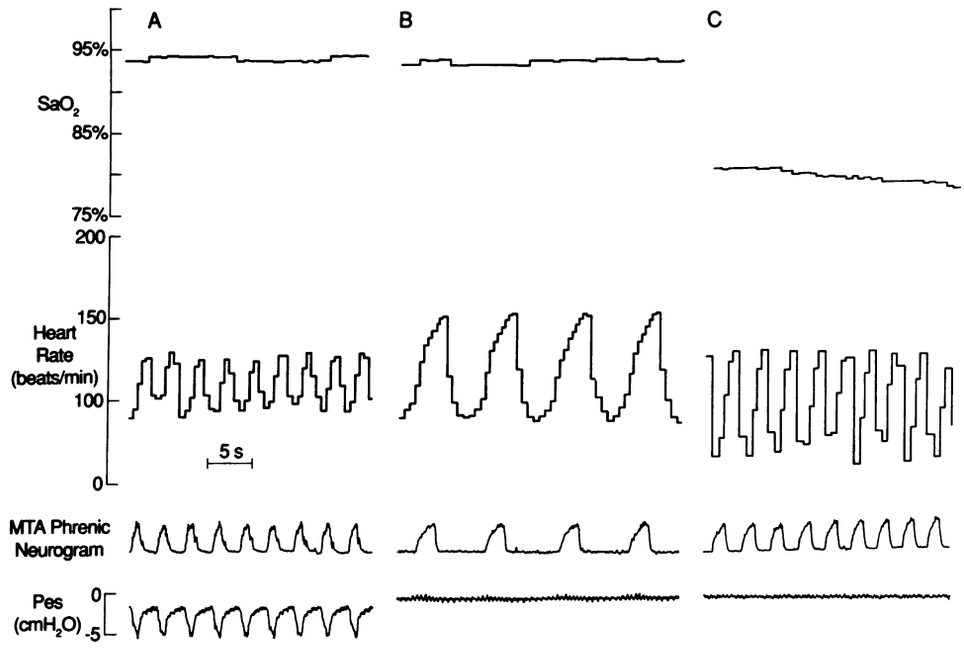

Figure 1. Sample data redrawn from chart recordings for progressive hypoxia. (*A*) Spontaneous breathing; (*B*) and (*C*) constant flow ventilation. *A* and *B* were selected to show similar oxygen saturations; however, the respiratory frequencies differ. *A* and *C* were selected to show similar respiratory frequencies; however, the oxygen saturations differ. The patterns were similar during progressive hypercapnia.

and the measures of chemostimulation, the slopes were different among conditions. The mean slopes±SD for the runs in which the coefficient of determination for the linear fit ("R squared") was greater than or equal to 0.80 for hypoxia were, in log (bpm/arbitrary unit)/log(percent saturation), for spontaneous breathing: −7.0±2.3, n = 6; and for CFV: −5.4±1.9, n = 7; and for hypercapnia were, in log (bpm/arbitrary unit)/log (Torr), for spontaneous breathing: −4.6±2.0, n = 7; and for CFV: −2.3±1.2, n = 7.

A sample plot of RSA_a amplitude against frequency is shown on the left in Fig. 3, and in log–log (Bode plot) form on the right. All runs in which there was a sufficient range of respiratory frequencies for calculations (34 of 36) had a linearly decreasing region in the log–log representation. Some also had a plateau at the lowest frequencies but this plateau extended over only a short frequency range. The mean slopes±SD of the down-going portions, in log (bpm/arbitrary units)/decade of frequency, for all runs in which the coefficient of determination for the linear fit was greater than or equal to 0.80 were, for hypoxia, spontaneous breathing: −1.9±0.4, n = 7; for hypoxia, CFV: −1.8±0.7, n = 7; for hypercapnia, spontaneous breathing: −2.1±0.8, n = 5; and for hypercapnia, CFV: −1.9±0.7, n

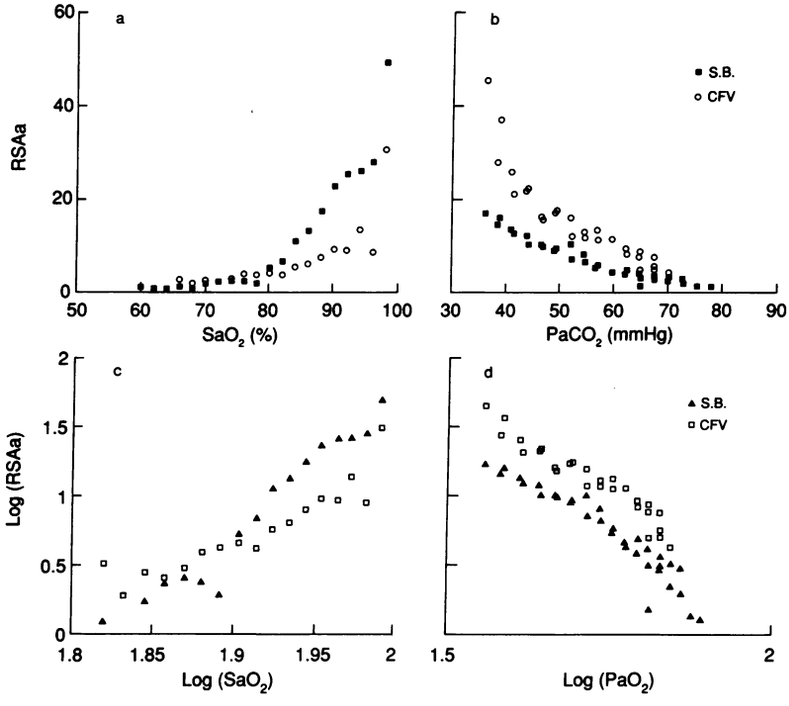

Figure 2. (*Top*) Adjusted RSA magnitude plotted against oxygen saturation or P_aCO_2 in one dog. (*Bottom*) Same data, log–log representation.

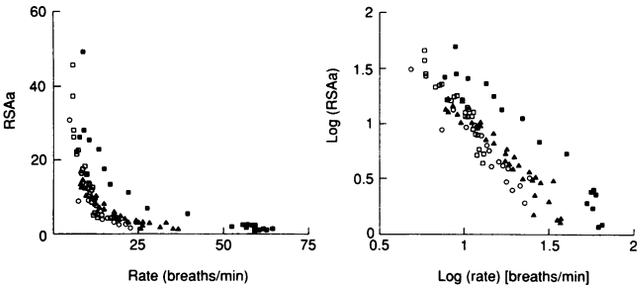

Figure 3. (*Left*) Adjusted RSA plotted against respiratory frequency for one dog. (*Right*) Same data, log–log representation. ■, SB O_2; ○, CFV O_2; ▲, SB CO_2; □, CFV CO_2.

= 4. A one way analysis of variance indicated that the log–log slopes of the four conditions are statistically indistinguishable ($P = 0.90$), and the global mean slope (−1.9) is not significantly different from −2.0. The intercept for spontaneous breathing with hypoxic stimulation is generally higher than those for the other experimental conditions, as it is in the example shown in the figure.

The pooled frequency responses (Fig. 4) show that RSA_a as a function of the onset of inspiration can be characterized as a slightly overdamped second order system. An additional, cascaded second order system with a higher corner frequency is suggested by the −80 dB/decade asymptote at the highest frequencies.

The precision of the parameters obtained for the second order system is necessarily low, since the pooled graphs show a moderate degree of scatter, rendering the position of the asymptotes and the intercepts somewhat subjective. However, differences can be seen among conditions. For hypoxic stimulation, the natural frequencies were 13 breaths/min for spontaneous breathing and 11 breaths/min with CFV, with corresponding damping parameters of 1.01 and 1.03. (The time constants were 1.0 s and 0.6 s for spontaneous breathing and 1.1 s and 0.7 s for CFV). For hypercapnic stimulation, the natural frequencies were lower. That for spontaneous breathing could not be obtained, as the dogs did not breathe slowly enough for the low frequency asymptote to be determined. However, the natural frequency can be estimated by eye to fall between 11 and 13 breaths/min. During CFV, the natural frequency was 8 breaths/min and the damping parameter was 1.05. (The time constants with CFV were 1.7 s and 1.0 s, and the faster time constant for spontaneous breathing was 0.5 s). The frequencies at which the additional system became evident were, for hypoxia, 32 breaths/min during spontaneous breathing and 22 breaths/min during CFV, and, for hypercapnia, 20 breaths/min for spontaneous breathing and 7 breaths/min during CFV.

Respiratory rates at the beginning of the runs varied, leading to different initial values of RSA. Thus, only the changes from baseline were considered in detail. However, a trend to a slightly greater RSA_a during spontaneous breathing than during CFV was noted; RSA_a at ~ 10 breaths/min was never less with spontaneous breathing than with CFV, and was greater in 10 of the 18 pairs of runs with similar chemostimulation.

Discussion

Heart rate modulation synchronous with phrenic neural activity was evident both in the presence of phasic afferents during spontaneous breathing and in their absence during CFV. This effectively rules out pulmonary stretch receptor afferents, cyclic baro- or mechanoreceptor afferents, cyclic oscillations in chemoreceptor afferents, or any other phasic afferent information as necessary for the generation of respiratory sinus arrhythmia. Furthermore, RSA_a was a similar function of frequency whether the changes were produced by normocapnic progressive hypoxia (peripheral chemoreceptors) or hyperoxic progressive hypercapnia (central chemoreceptors), indicating that the direct influence of the chemoreceptors on the system that produces the modulation in phase with respiration is minor, but that most of their effect on RSA is through their effects on respiratory drive.

Our data show that phasic afferent signals are not necessary for the generation of respiratory sinus arrhythmia and that when they are present their effects are minimal. In the second conclusion we appear to differ from Anrep et al. (14) who showed that the magnitudes of heart rate fluctuation caused by

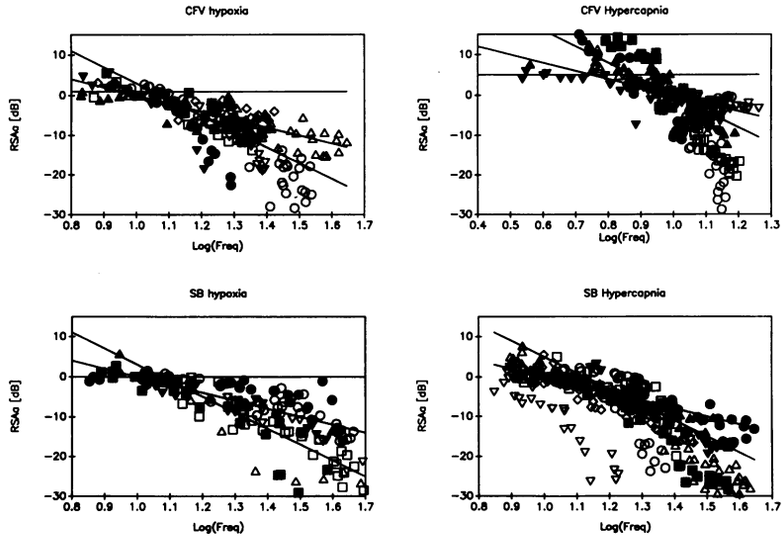

Figure 4. Pooled frequency responses for all dogs. Different symbols represent different animals. Lines of slope 0 dB/decade, −20 dB/decade, and −40 db/decade are included.

reflex stimulation could equal that caused by respiratory drive. However, Anrep et al. did not consider the magnitude of the stimuli necessary to generate the heart rate changes, and the invasive nature of their investigation may have altered the system sensitivity. Furthermore, those investigators considered the central and reflex phenomena separately, and they are probably not purely additive when simultaneous. For example, the MTA phrenic neurogram amplitude is lower during CFV than during spontaneous breathing (15), as is the amplitude of RSA, suggesting that one of the ways that phasic afferents may augment RSA in the intact animal is by augmenting ventilatory drive. The ratio of RSA magnitude to the amplitude of the MTA phrenic neurogram during hypercapnic stimulation was unchanged by the presence of phasic afferents.

The magnitudes of RSA were adjusted by division by the amplitude of the MTA phrenic neurogram to yield RSA_a. This step is inherent in the description of RSA as being driven by the respiratory signal since the output magnitude divided by the input magnitude yields the gain of a system. RSA amplitude has been shown to be linearly related to tidal volume at moderate lung volumes (5, 6), and the amplitude of the MTA phrenic neurogram is proportional to tidal volume (16).

The slope of log (RSA_a) vs. log (frequency), -1.9 log (bpm/arbitrary unit)/decade, was statistically indistinguishable from -2, or a slope of -40 dB per decade, the asymptotic slope of a second order lowpass system. The deviations from the value of -2 are consistent with the second order model, resulting most probably from proximity to the corner frequency; the asymptotic slope is not achieved in general until a frequency about five times greater than the breakpoint, while our range of frequencies spanned only about a fourfold increase.

We have not proven that the system is second order and linear, but we have shown that it is the simplest system consistent with the data. Although others (16) working with human subjects assumed a first order system, their data are not inconsistent with the higher order model. The highest breathing frequencies achieved voluntarily by their subjects were simply too close to the natural frequency for a steeper roll-off to have been evident even if it had been present. A relatively complex model of the mechanism by which the cardiac period is affected by the frequency of vagal discharge (17) is second order on the rate of change in vagal tone for a moderate range of, and small fluctuations in vagal discharge.

The damping ratio of the system as measured here was not clearly affected by the presence of phasic afferents nor by the nature of the stimulus causing the increase in respiratory drive, although small differences could have been masked by the error of measurement. The natural frequency of the system appeared to be lower with hyperoxic hypercapnia than with normocapnic hypoxic stimulation, and for CFV than for spontaneous breathing. However, these results, too, are within the error of our parameter detection. The scatter in the data was not reduced if the respiratory frequency was divided by the mean heart rate. As we have shown previously, heart rate increased under hypoxic conditions during spontaneous spontaneous breathing but decreased during CFV (18).

Results obtained in some experiments with human subjects have been interpreted as showing no direct central neural generation of RSA, but rather an adjustment of the baroreflex giving rise to the phenomenon (19). Our findings in dogs differ, in that the elimination of the large intrathoracic pressure fluctuations associated with breathing did not alter RSA, which remained related to the MTA phrenic neurogram. This major discrepancy could be due to interspecies differences, to effects of anesthesia, or to incomplete suppression of respiratory drive in the human experiments. It is possible that the anesthetic agent in our experiment could have eliminated an inhibiting effect that was present in the conscious animal. However, in light of our data, it is more likely that respiratory drive was not completely eliminated in the human experiments. The ventilated dogs in our experiments showed neural ventilatory activity even when they were hyperoxic and normocapnic on CFV, that is, in the absence of obvious stimuli for breathing. Similarly, despite their efforts to relax their respiratory muscles and to let the cuirass respirator ventilate them, the human subjects in Melcher's study may have had a "respiratory drive" signal; it is not clear where in the pathways that generate the pattern of breathing the higher centers act, nor precisely where the signal that is seen as vagal output to the heart is tied to the respiratory center. It is also possible that central projection of the respiratory drive directly modulates the baroreflex rather than the cardiac controller. In this case, stimulation of the baroreflex with thoracic pressure swings or modulation of it centrally could have similar effects. Our data show fluctuations of arterial pressure corresponding to the respiratory sinus arrhythmia, fluctuations that may be caused by the heart rate changes or may cause them. Levy and colleagues (20) showed that respiratory sinus arrhythmia was measurable in a preparation in which the arterial pressure to both the coronary bed and the cephalic portion of the animal was held constant and nonpulsatile, and the venous return was kept constant. Because respiratory sinus arrhythmia can be produced in the absence of blood pressure fluctuations, we conclude that the respiratory modulating activity acts directly on the cardiac controller. We do not exclude the possibility that it also may modulate barocenter activity simultaneously.

Our findings that the system can be described as linear and second order and that the order (roll-off) of the system is independent of blood gas values differ somewhat from those of other authors (3, 4). However, the experimental situations were significantly different. First, our data were obtained in anesthetized dogs, not in conscious humans. Second, the frequency changes in our experiments were caused by altered blood gases, rather than being selected voluntarily. Thus, we avoided any confounding effects of higher centers on spontaneous breathing, but with our protocol there were different blood gases at each frequency. If carotid body afferents modify the natural frequency in the second order model, we will have seen a sum of multiple response curves during hypoxia. During hypercapnia when the carotid body afferents were reduced by the use of hyperoxia (21), we may have seen a sum of curves for different levels of central chemoreceptor activity. These relatively minor effects would be evident only near the natural frequency of the system, giving rise to some blurring of the response near the corner.

Over the range of our measurements, the RSA–respiration system magnitude response, if linear, appears to be second order. Thus, one might expect to find a physical system analogous to an RLC circuit, that is, with resistance, capacitance, and inductance as the source of the phenomenon. However, a central (neural) model with these components and time constants of the order of seconds is difficult to envisage. The possi-

bility that the signal is in fact a pressure artifact can be ruled out; RSA is as clear on heart rate signals generated from ECG records as it is on those from pulse registration. However, the physical nature of the second order system is elusive.

In our attempt to locate a putative generator for RSA, we examined the process by which the signal is transmitted and detected, with very interesting results. It appears that the frequency behavior of RSA can be accounted for to a large extent by features of signal transmission, without recourse to any linear system model. RSA amplitude is defined as the difference between maximum and minimum heart rate over one breathing period. In other words, RSA is the maximum deviation of the frequency of cardiac contraction occurring at the respiratory frequency. It can be considered, then, that a signal related to breathing is transmitted by frequency modulation (FM) of the mean heart rate. However, the frequency of the carrier, the mean heart rate, is only five to six times higher than the frequency of the modulating signal, the breathing rate.

The carrier in an FM system is an oscillating signal with a fixed mean frequency. The modulating signal is encoded as perturbations of the carrier frequency, with the instantaneous amplitude of the transmitted signal mapped onto the magnitude of the deviation from the mean frequency and the frequency of the transmitted signal mapped onto the frequency of the perturbations. A modulating period includes many carrier cycles and the variations in frequency occur smoothly when the carrier frequency is much greater than the modulating frequency. However, the frequency and amplitude information begin to interfere with one another if the two frequencies approach each other too closely.

We propose a simplified model of RSA as an FM phenomenon. The carrier frequency is a constant mean heart rate. The modulating signal is respiratory suppression of the vagal input to the cardiac (or pressure-regulating) center. For simplicity, consider both signals to be sinusoidal, unless the baseline vagal tone is low enough that the respiratory suppression forces it to zero before the end of inspiration. In the modulated signal, then, the maximum deflections from the mean heart rate will be proportional to the tidal volume. If the breathing rate is low, the largest tidal volume that can be carried is the one that either forces the heart rate or the vagal input to the heart to zero. If the tidal volume is very small then the frequency limit for the modulating signal is half the carrier frequency, to allow one carrier cycle for the minimum and one for the maximum of the modulating signal.

Broadly speaking, the bandwidth around the carrier frequency needed for FM transmission of any modulating signal is twice the sum of the modulating frequency and the maximum frequency deflection to occur. For the simplified RSA transmission model discussed here, the breathing frequency plus the gain-tidal volume product must be less than the mean heart rate or the amplitude of the breathing signal will be attenuated in transmission. The frequency of breathing at which attenuation (because of the limitations of frequency modulation) becomes apparent will depend on the system gain and the mean heart rate.

The model described above has been developed in more detail in the Appendix, and results of a simulation of this system are shown in Fig. 5. A plot of simulated RSA amplitude in decibels vs. log (f_m) is given in Fig. 6 for constant tidal volume, f_c, and system gain. For small tidal volumes and system gains

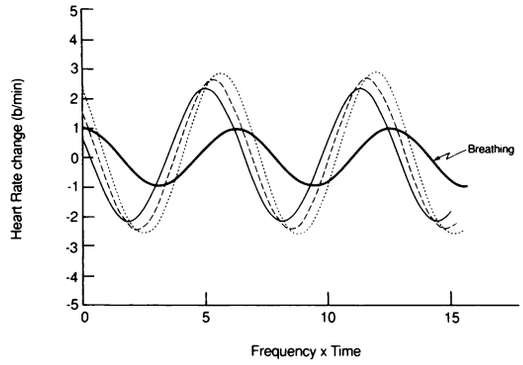

Figure 5. Simulation results of heart rate vs. time for sinusoidal variations (Eq. A6). The respiratory signal is shown for reference. Note the phase changes that occur with frequency. ------, 12/min; – – –, 18/min; ——, 24/min.

there is an approximately linear relationship between RSA magnitude and tidal volume (Eq. A7), but not for higher gain-tidal volume products, a phenomenon that has been reported for RSA in man (5, 6). The phase relation between RSA and breathing is a function of frequency (Fig. 5), as has been seen by others (3, 7). The similarity of Fig. 6 to the RSA_a data plots is striking if a narrow range of frequency ratios is selected. This is especially noteworthy because there is no physical system involved here, but simply a nonlinear signal transmission process.

The FM transmission model permits the inclusion of several secondary effects. Changes in f_c alter the apparent f_n of the second order fit to the model, perhaps explaining the secondary effects of chemoreceptors on RSA as direct effects on heart rate (f_c in the model). System gain and baseline vagal tone might vary with subject age and with presence or absence of phasic afferents.

This model does not, as yet, account for the nonsinusoidal nature of the signals nor the threshold caused by the baseline vagal tone. The discontinuous nature of the heart rate signal has been addressed for a different purpose in a recent model (22), but further work remains to be done.

The roll-off pattern of RSA_a in anesthetized dogs is consistent with the limitations of a frequency-modulated system with a low frequency carrier, a nonlinear description in which no particular circuit elements need be involved. However, RSA_a can be described as an overdamped second order system. Exper-

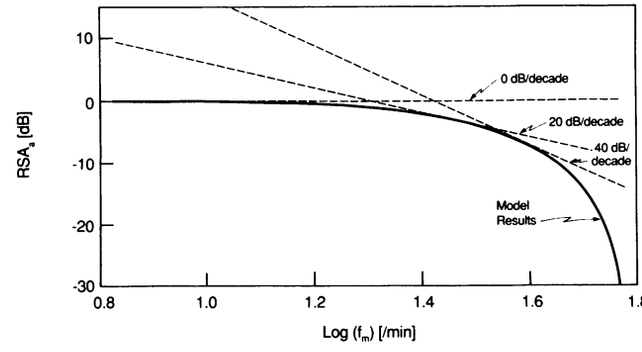

Figure 6. Bode plot of model. Lines of slope 0 dB/decade, −20 dB/decade, and −40 db/decade are included.

imental data show RSA_a to be independent of phasic afferent and chemoreceptor inputs, and to depend primarily on the frequency of respiratory drive.

Appendix

If we approximate the cardiac contraction signal, the carrier, as a sinusoidal function

$$c(t) = \cos(2\pi f_c t) \tag{A1}$$

where f_c is the mean unmodulated heart rate, and assume that it is modulated by a second sinusoidal signal at the respiratory rate,

$$r(t) = aV_T \cos(2\pi f_m t) \tag{A2}$$

where f_m is the modulating breathing frequency, we can express the transmitted pulse waveform as

$$p(t) = \cos[2\pi f_c t + KV_T/f_m \sin(2\pi f_m t)] \tag{A3}$$

where K V_T/f_c is the modulation parameter, directly proportional to tidal volume and inversely proportional to f_c. The biotachometer detects maxima of p(t), producing as output the inverse of the interval from the last maximum, the instantaneous heart rate. Hence,

$$HR(t) = 1/(t_2 - t_1) \tag{A4}$$

where t_2 and t_1, the occurrences of the maxima, are defined by

$$2\pi f_c(t_2 - t_1) + KV_T[\sin(2\pi f_m t_2) - \sin(2\pi f_m t_1)] = 2\pi \tag{A5}$$

This equation can be rearranged to give

$$HR(t) = f_c/\{1 - KV_T/(\pi f_m) \cos[2\pi f_m(t_1 + \Delta t/2)] \sin(\pi f_m \Delta t)\} \tag{A6}$$

where $\Delta t = t_2 - t_1$, the interval between two heart beats.

RSA amplitude is defined as the difference between maximum and minimum over one breathing period, i.e., from the time when the f_m term equals 1 to the time when it equals -1. If the variations in heart rate are small, $\Delta t = 1/f_c$, and

$$RSA = 2KV_T f_c/\pi f_m \sin(\pi f_m/f_c)/ [1 - (KV_T/(\pi f_m)^2 \sin^2(\pi f_m/f_c)] \tag{A7}$$

A sample plot of log (RSA) vs. log (f_m) based on Eq. A7 is given in Fig. 6. The phase behavior is indicated in Fig. 5 by a plot of Eq. A6, heart rate as a function of time for different values of f_m.

Acknowledgments

The authors thank Mrs. Elena Mates for her technical assistance.

This work was partially supported by the Heart and Stroke Foundation and the Medical Research Council of Canada.

References

1. Ludwig, C. 1847. Beitrage zur Kenntniss des Einflusses der Respirationsbewegungen auf den Blutlauf in Aortensysteme. *Arch. Anat. Physiol. wissen. Med.* 13:240–302.

2. Hamlin, R. L., C. R. Smith, and D. L. Smetzer. 1966. Sinus arrhythmia in the dog. *Am. J. Physiol.* 210:321–328.

3. Selman, A., A. McDonald, R. Kitney, and D. Linkens. 1982.The interaction between heart rate and respiration. Part I. Experimental studies in man. *Automedica (Lond.).* 4:131–139.

4. Hirsch, J. A., and B. Bishop. 1981. Respiratory sinus arrhythmia (RSA) in man: altered inspired O_2 and CO_2. *In* Advances in Physiological Science. Vol. 9. Cardiovascular Physiology. Neural Control Mechanism. A. G. B. Kovach, P. Sandor, and M. Kollai, editors. Pergamon Press, Elmsford, NY. pp. 305–312.

5. Eckberg, D. L. 1983. Human sinus arrhythmia as an index of vagal cardiac outflow. *J. Appl. Physiol.* 54:961–966.

6. Hirsch, J. A., and B. Bishop. 1981. Respiratory sinus arrhythmia in humans: how breathing pattern modulates heart rate. *Am. J. Physiol.* 241:H620–H629.

7. Angelone, A., and N. A. Coulter. 1964. Respiratory sinus arrhythmia: a frequency dependent phenomenon. *J. Appl. Physiol.* 19:479–482.

8. Band, D. M., C. B. Wolf, J. Ward, G. M. Cochrane, and J. Prior. 1960. Respiratory oscillations in arterial carbon dioxide as a control signal in exercise. *Nature (Lond.).* 285:83–85.

9. Watson, J. W., D. R. Burwen, R. D. Kamm, R. Brown, and A. S. Slutsky. 1986. Effect of flow rate on blood gases during constant flow ventilation in dogs. *Am. Rev. Respir. Dis.* 133:626–629.

10. Slutsky, A. S., and A. S. Menon. 1987. Catheter position and blood gases during constant flow ventilation. *J. Appl. Physiol.* 62:513–519.

11. Lehnert, B. E., G. Oberdorster, and A. S. Slutsky. 1982. Constant flow ventilation of apneic dogs. *J. Appl. Physiol.* 53:483–489.

12. Smyth, R. J., A. D. D'Urzo, A. S. Slutsky, B. M. Galko, and A. S. Rebuck. 1986. Ear oximetry during combined hypoxia and exercise. *J. Appl. Physiol.* 60:716–719.

13. Reeves, R. B., J. S. Park, G. N. Lapennas, and A. J. Olszowka. 1982. Oxygen affinity and Bohr coefficients of dog blood. *J. Appl. Physiol.* 38:87–96.

14. Anrep, G. V., W. Pascual, and R. Rossler. 1936. Respiratory variations of the heart rate. II. The central mechanism of the respiratory arrhythmia and the inter-relations between the central and the reflex mechanisms. *Proc. R. Soc. Lond. B Biol. Sci.* 119:218–232.

15. Naqvi, S. S. J., A. S. Menon, B. E. Shykoff, A. S. Rebuck, and A. S. Slutsky. 1991. Phrenic neural output during hypoxia in dogs. Constant flow ventilation (CFV) vs. spontaneous breathing. *J. Appl. Physiol.* In press.

16. Eldridge, F. L. 1971. Relationship between phrenic nerve activity and ventilation. *Am. J. Physiol.* 221:535–543.

17. Negoescu, R. M., and I. E. Csiki. 1989. Model of respiratory sinus arrhythmia in man. *Med. & Biol. Eng. & Comput.* 27:260–268.

18. Kato, H., A. S. Menon, and A. S. Slutsky. 1988. Mechanisms mediating the heart rate response to hypoxemia. *Circulation.* 77:407–414.

19. Melcher, A. 1976. Respiratory sinus arrhythmia in man: a study in heart rate regulating mechanics. *Acta Physiol. Scand.* 435(Suppl.):1–31.

20. Levy, M. N., H. DeGeest, and H. Zieske. 1966. Effects of respiratory center activity on the heart. *Circ. Res.* 18:67–78.

21. Lahiri, S., and R. G. Delaney. 1975. Stimulus interaction in the responses of carotid body chemoreceptor single afferent fibers. *Respir. Physiol.* 24:249–266.

22. Witte, H., and M. Rother. 1989. Better quantification of neonatal respiratory sinus arrhythmia. Progress by modeling and model-related physiological examinations. *Med. & Biol. Eng. & Comput.* 27:298–306.